

Theory of Spin Glass by the Method of the Distribution Function of an Effective Field

Shigetoshi KATSURA

Department of Applied Physics, Tohoku University, Sendai 980
and

Faculty of Science and Engineering, Tokyo Denki University
Hatoyama, Saitama 350-03^{)}*

(Received September 13, 1986)

The theory of the random Ising model formulated in terms of the distribution function of the effective field in the pair and in the cluster approximations is reviewed. An integral equation for the distribution function is derived. The integral equation has a solution for the paramagnetic state, a solution for the ferromagnetic state, a solution for the antiferromagnetic state, and solutions for the spin glass state.

The phase diagram, and the ground state energy and entropy are calculated. The ground state entropy of the model is shown to be a small positive quantity contrary to the Sherrington-Kirkpatrick infinitely long-ranged model.

The phase diagram derived from the cluster approximation well explains the experimental phase diagrams, in particular, of fcc spin glass and the spin glass of $\text{Eu}_p\text{Sr}_{1-p}\text{S}$.

The distribution function for the spin glass in the pair approximation at $T=0$ with a continuous distribution is obtained analytically. They are composed of δ -functions or of δ -functions and a quadratic continuous function.

§ 1. Introduction

In this paper the treatment of random spin systems, especially of the spin glass problem by the method of the distribution function of the effective field developed by our group is reviewed. A cluster (pair, triangle, square, tetrahedron, etc.) is taken in a given lattice (square, triangle, simple cubic, hexagonal, face-centered cubic, etc.). An effective field with a distribution is assumed to be applied to each vertex of the cluster. The partition function of the cluster is calculated exactly in terms of these effective fields. Self-consistent relation leads to an integral equation for the distribution function of the effective fields. The solution of the integral equation gives the physical quantities, the phase diagrams and the ground state properties.

We consider random Ising models on a given crystal lattice. The hamiltonian \mathcal{H} , the density matrix ρ , and the free energy F are given by

$$\mathcal{H}(\{H_i, J_{ij}\}) = - \sum_{\langle ij \rangle} J_{ij} \sigma_i \sigma_j - \sum_i H_i \sigma_i, \quad H_i = m_i H, \quad (1.1)$$

$$\rho(\{H_i, J_{ij}\}) = \exp[-\beta \mathcal{H}(\{H_i, J_{ij}\})], \quad (1.2)$$

$$-\beta F = \int \ln \text{tr} \rho(\{H_i, J_{ij}\}) \prod P(J_{ij}) dJ_{ij}. \quad (1.3)$$

^{*)} Present address.

where $i(=1, 2, \dots, N)$ denotes a site of the given crystal lattice, H_i the external field, and $\langle ij \rangle$ the pair of sites i and j . Random models are classified into bond-random and site-random models.

1) In the bond-random model, J_{ij} distribute with a distribution $P(J)$, and the magnetic moments m_i are equal for all i and we put $m_i=1$. The bond-random model is further classified into 1a) nearest-neighbor model (in general, short-ranged model), and 1b) infinitely long-ranged model. In 1a) $P(J)$ is given by

$$P(J_{ij}) = p_A \delta(J_{ij} - J_A) + p_B \delta(J_{ij} - J_B) \tag{1.4}$$

for the nearest-neighbor pair ij (A and B are species of the bonds).

2) In the site-random model, m_i is m_A or m_B , with the distribution (A and B are species of the sites)

$$P(m_i) = p_A \delta(m_i - m_A) + p_B \delta(m_i - m_B). \tag{1.5}$$

J_{ij} is J_{AA} , J_{BB} , or J_{AB} according as i and j are of species A and A, B and B , or A and B .

In such systems there appears the spin glass state where spins are frozen, besides the ferro-, antiferro- and paramagnetic states, when the interactions are competing.^{1)~3)}

The problem is formulated^{3)~7)} in the scheme of an integral equation for the distribution function of an effective field. The boundaries between the paramagnetic, ferromagnetic, antiferromagnetic and spin glass states are determined as functions of the concentration of the ferromagnetic bond and the ground state energy and entropy are obtained. Some discussions are given of the results.

§ 2. The integral equation in the pair approximation

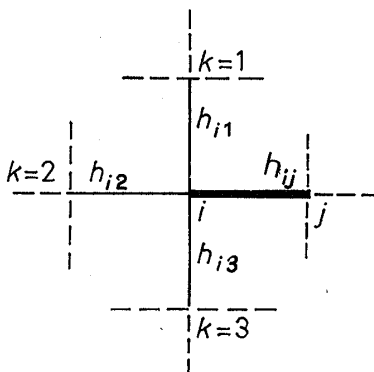


Fig. 1. Pair cluster in the lattice.

$$h_{i1} + h_{i2} + h_{i3} = H_{i-ij}^{(2)}, \quad h_{i1} + h_{i2} + h_{i3} + h_{ij} = H_i^{(1)}.$$

We consider a system of Ising spins for which the distribution of exchange integrals J_{ik} is given by (1.4). The system is treated in the pair (Bethe) approximation. We take a pair ij in the lattice. The effective field on the spin i due to its neighboring spin k is denoted by h_{ik} , and called the single-bond field. The one-body and two-body density matrices $\rho_i^{(1)}$ and $\rho_{ij}^{(2)}$ are given by

$$\rho_i^{(1)} = \exp(\beta H_i^{(1)} \sigma_i), \tag{2.1}$$

$$\rho_{ij}^{(2)} = \exp[\beta (H_{i-ij}^{(2)} \sigma_i + H_{j-ij}^{(2)} \sigma_j + J_{ij} \sigma_i \sigma_j)], \tag{2.2}$$

$$H_i^{(1)} = \sum_k h_{ik} + H_i,$$

$$H_{i-ij}^{(2)} = \sum_{k(\neq j)} h_{ik} + H_i. \tag{2.3}$$

$H_{i-ij}^{(2)}$ is the effective field at the spin i from the outside of the pair ij . $H_{i-ij}^{(2)}$ is simply denoted by $H_i^{(2)}$ hereafter and called the two-body effective field (Fig. 1). The partial trace of $\rho_{ij}^{(2)}$ with respect to j is given by

$$\text{tr}_j \hat{\rho}_{ij}^{(2)} = \frac{\exp\{[\beta H_i^{(2)} + \text{th}^{-1}(\text{th} \beta J_{ij} \text{th} \beta H_j^{(2)})] \sigma_i\}}{2 \text{ch}[\beta H_i^{(2)} + \text{th}^{-1}(\text{th} \beta J_{ij} \text{th} \beta H_j^{(2)})]}, \quad (2.4)$$

where $\hat{\rho}$ denotes the corresponding normalized quantity. We postulate that physical quantities derived from the one-body and reduced two-body density matrices are equal on the average. The reducibility $\hat{\rho}_i^{(1)} = \text{tr}_j \hat{\rho}_{ij}^{(2)}$ leads to

$$\beta H_i^{(1)} = \beta H_i^{(2)} + \text{th}^{-1}(\text{th} \beta J_{ij} \text{th} \beta H_j^{(2)}).$$

Eliminating $H_i^{(1)}$ with the use of (2.3), we have a set of N equations among the two-body effective fields $H_i^{(2)}$. From those equations we can derive Thouless-Anderson-Palmer equation.^{8),9)} Instead of solving the N equations we consider a distribution function $G_i^{(2)}(H_i^{(2)})$ of the two-body effective field $H_i^{(2)}$. In the states such as the paramagnetic, ferromagnetic, or spin glass states, we regard that the distribution of the effective field is independent of the site. Then the subscript i of G_i is dropped and we have an integral equation^{3),4)} for $G^{(2)}(H^{(2)})$:

$$G^{(2)}(H_i^{(2)}) = \int \delta(H_i^{(2)} - H - (1/\beta) \sum'_{k(\neq j)} \text{th}^{-1}(\text{th} \beta J_{ik} \text{th} \beta H_k^{(2)})) \times \prod'_{k(\neq j)} [P(J_{ik}) dJ_{ik} G^{(2)}(H_k^{(2)}) dH_k^{(2)}]. \quad (2.5)$$

Here \sum' and \prod' denote the sum and product over $z-1$ nearest-neighbors of i excluding j . $\int_{-\infty}^{\infty} \dots \int_{-\infty}^{\infty}$ is simply denoted by \int .

By using Fourier transform, (2.5) is transformed into simultaneous integral equations:

$$G^{(2)}(H^{(2)}) = \frac{1}{2\pi} \int dx \exp[ix(H^{(2)} - H)] [S(x)]^{z-1}, \quad (2.6)$$

$$S(x) = \int dH^{(2)} G^{(2)}(H^{(2)}) dJ P(J) \exp[-i(x/\beta) \text{th}^{-1}(\text{th} \beta H^{(2)} \text{th} \beta J)]. \quad (2.7)$$

Here the imaginary unit i appears which must not be confused with label i for a site. When we put $P(J) = \delta(J - J_0)$, then we have a fundamental equation for the Bethe approximation of the Ising ferromagnet:¹⁰⁾

$$\beta H^{(2)} = \beta H + (z-1) \text{th}^{-1}(\text{th} \beta J_0 \text{th} \beta H^{(2)}). \quad (2.8)$$

Equation (2.8) for $z=2$ gives the exact solution of the one-dimensional Ising model.

Further, substituting (2.6) into (2.7), we have¹¹⁾

$$S(x) = (1/2\pi) \int dx K(x, y) [S(y)]^{z-1}, \quad (2.9)$$

$$K(x, y) = \int dJ dH^{(2)} P(J) \exp\{iy(H^{(2)} - H) - i(x/\beta) \text{th}^{-1}(\text{th} \beta H^{(2)} \text{th} \beta J)\}. \quad (2.10)$$

(2.9) is a standard form of the nonlinear integral equation. When $S(x)$ is solved, the distribution function $G^{(1)}(H^{(1)})$ of the one-body effective field $H_i^{(1)}$ is given by

$$G^{(1)}(H_i^{(1)}) = \frac{1}{2\pi} \int dx \exp[ix(H_i^{(1)} - H)] [S(x)]^z. \quad (2.11)$$

$S(x)$ is the Fourier transform of the distribution function $g(h)$ of the single-bond effective field h_{ik} :

$$g(h) = \frac{1}{2\pi} \int dx \exp[ix(h-H)] S(x). \tag{2.12}$$

The magnetization σ and the spin-glass order parameter q are given by*

$$\sigma = \int dH^{(1)} \text{th} \beta H^{(1)} G^{(1)}(H^{(1)}), \tag{2.13}$$

$$q = \int dH^{(1)} \text{th}^2 \beta H^{(1)} G^{(1)}(H^{(1)}). \tag{2.14}$$

When the external magnetic field H is zero, the paramagnetic state is characterized by $\sigma=0$ and $q=0$, the ferromagnetic state by $\sigma \neq 0$ and $q \neq 0$, and the spin glass state by $\sigma=0$ and $q \neq 0$. Instead of σ and q we can use³⁾ \bar{l} and \bar{l}^2 ($\bar{l} \equiv \text{th} \beta H^{(2)}$).

§ 3. Uniform and spin glass susceptibilities in the pair approximation

We consider the paramagnetic region taking up to the leading order of the effective field. We calculate the uniform and spin glass susceptibilities. Multiplying $H_i^{(2)n}$ to both sides of (2.5), and integrating with respect to $H_i^{(2)}$, we have

$$\overline{H_i^{(2)n}} = \int \delta(H_i^{(2)} - H - \sum'_k h_{ik}) H_i^{(2)n} dH_i^{(2)} \prod'_k P(J_{ik}) dJ_{ik} \prod'_k G^{(2)}(H_k^{(2)}) dH_k^{(2)}, \tag{3.1}$$

where $n=1$ or 2 , k takes the $z-1$ sites of nearest-neighbors of i excluding j , and

$$\beta h_{ik} = \text{th}^{-1}(\text{th} \beta J_{ik} \text{th} \beta H_k^{(2)}). \tag{3.2}$$

Here we denote the average over $P(J_{ij})$ and $G^{(2)}(H_k^{(2)})$ by $\overline{\quad}$. Carrying the integration in (3.1), we have up to the order $O(h^n)$

$$\overline{H_i^{(2)n}} = \overline{(H + \sum'_k h_{ik})^n} = H^n + \overline{\sum'_k h_{ik}^n} \simeq H^n + (z-1) \overline{h_{ik}^n}, \tag{3.2'}$$

where we regard h as a small quantity and the cross terms as higher order quantities, i.e.,

$$\overline{h_{ik}^n h_{ik'}^n} = \overline{h_{ik}^n} \overline{h_{ik'}^n} = O((h^n)^2), \quad (k' \neq k'')$$

are discarded.

We insert (3.2) into (3.2'). Then

$$\overline{H_i^{(2)n}} = H^n + (z-1) \overline{\left[\frac{1}{\beta} \text{th}^{-1}(t_{ik} l_k) \right]^n} = H^n + (z-1) \overline{t_{ik}^n} \overline{H_k^{(2)n}}, \tag{3.3}$$

where $t_{ik} \equiv \text{th} \beta J_{ik}$. Similarly

$$\overline{H_i^{(1)n}} = H^n + z \overline{\left[\frac{1}{\beta} \text{th}^{-1}(t_{ik} l_k) \right]^n} = H^n + z \overline{t_{ik}^n} \overline{H_k^{(2)n}}. \tag{3.4}$$

Hence the uniform and spin glass susceptibilities

$$\chi_u/\beta = \partial\sigma/\partial H \simeq \partial\overline{H^{(1)}}/\partial H \quad \text{and} \quad \chi_g/\beta^2 = \partial q/\partial(H^2) \simeq \partial\overline{H^{(1)2}}/\partial(H^2)$$

in the high temperature region are given by

*) The order parameter of the random ordered phase¹²⁾ ξ is given by

$$\xi = \int dH^{(1)} \text{th} \beta H^{(1)} G^{(1)}(H^{(1)}).$$

$$\chi_u/\beta = \frac{1 + \overline{\text{th } \beta J}}{1 - (z-1)\overline{\text{th } \beta J}}, \quad (3.5)$$

$$\chi_g/\beta^2 = \frac{1 + \overline{\text{th}^2 \beta J}}{1 - (z-1)\overline{\text{th}^2 \beta J}}. \quad (3.6)$$

When the lattice can be divided into two equivalent sublattices α and β , $G^{(2)}(H_i)$ is either $G_\alpha^{(2)}(H_i)$ or $G_\beta^{(2)}(H_i)$, according as i belongs to α or β . Applying a staggered field $H_\alpha = -H_\beta = H$, we can treat the antiferromagnetic state. For details, see Ref. 4).

In the case of the model given by (1.4) the transition temperatures are given by

$$1 \mp (z-1)(p_A t_A^n + p_B t_B^n) = 0, \quad t_A \equiv \text{th } \beta J_A, \quad t_B \equiv \text{th } \beta J_B. \quad (3.7)$$

Upper and lower signs with $n=1$ give the Curie and Néel temperatures, T_c and T_N , respectively. Upper sign with $n=2$ gives the spin glass transition temperature T_g . That is, for the $\pm J$ model, they are given by

$$\begin{aligned} \beta_c J &= \text{th}^{-1}[(z-1)/(2p-1)], \\ \beta_g J &= \text{th}^{-1}(z-1)^{1/2}, \\ \beta_N J &= \text{th}^{-1}[(z-1)/(1-2p)]. \end{aligned} \quad (3.7')$$

($\beta_c = 1/k_B T_c$, etc.)

The transition point β_g can be characterized as the point at which the nonlinear susceptibility $\chi_2 \equiv \partial^2 \chi_u / \partial H^2$ diverges.^{13)~15)} In the system of binary mixture, the phase boundary is obtained^{3),6)} as shown in Fig. 2. An explanation of the boundaries between the ferromagnetic and spin glass states is given in § 6.

The free energy for the $\pm J$ model in the pair approximation is given by^{16),17)}

$$F = (1-z)F^{(1)} + \frac{z}{2}F^{(2)}, \quad (3.8)$$

where

$$-\beta F^{(1)} = \overline{\ln \text{tr } \rho_i^{(1)}} \quad (3.9)$$

$$= \int \ln [2 \text{ch } \beta H^{(1)}] G^{(1)}(H^{(1)}) dH^{(1)}, \quad (3.9')$$

$$-\beta F^{(2)} = \overline{\ln \text{tr } \rho_{ij}^{(2)}} \quad (3.10)$$

$$\begin{aligned} &= \int \ln \{ \exp[\beta(-J + H_i^{(2)} + H_j^{(2)})] + \exp[\beta(-J - H_i^{(2)} - H_j^{(2)})] \\ &+ \exp[\beta(J + H_i^{(2)} - H_j^{(2)})] + \exp[\beta(J - H_i^{(2)} + H_j^{(2)})] \} G^{(2)}(H_i^{(2)}) G(H_j^{(2)}) dH_i^{(2)} dH_j^{(2)}. \end{aligned} \quad (3.10')$$

When $-\beta F$ is expanded in the form $-\beta F = \beta a + b + O(\beta^{-1})$, then the ground state energy

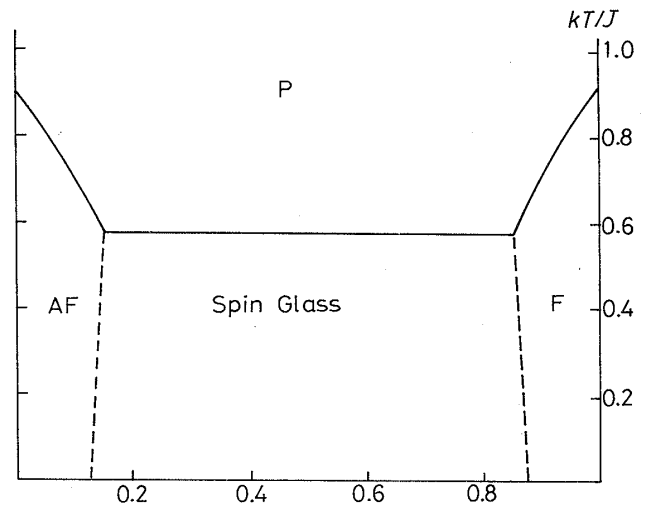


Fig. 2. Phase diagram of the $\pm J$ model in the pair approximation ($z=3$).

$$\begin{aligned} \text{th}(J/k_B T_c) &= 1/(2p-1)(z-1), \\ \text{th}^2(J/k_B T_g) &= 1/(z-1), \quad p_{FG} = 7/8. \end{aligned}$$

E and entropy S are given by $E = -a$ and $S/k_B = b$.

§ 4. Integral equation for the distribution function of the effective field in the cluster approximation

As shown in Fig. 2, the phase diagram of the $\pm J$ model in the pair approximation is symmetric with respect to the ferromagnetic and antiferromagnetic states. Though it can be made asymmetric by considering the $J_A - J_B$ model, many of real spin glass phase diagrams do not have either ferro- or antiferromagnetic state. Most of these substances have face-centered cubic structure. The frustration in the triangular and tetrahedron cluster as a unit of the fcc lattice is quite different from that in the square, cube, or hexagon clusters in the square, simple cubic, or hexagonal lattices.

In order to treat such an effect, we have developed cluster approximations. They are classified into a simple version and a full version. The former gives an exact solution for the cactus lattice and is called the cluster approximation simply. The latter is a generalization of Kikuchi's cluster variation method^{18)~20)} to random systems. Here we treat the former approximation. For the latter treatment see Ref. 21).

We approximate the lattice by an appropriate cactus lattice composed of clusters (pair, triangle, square, tetrahedron, etc.), z_c of which $(ijkl\cdots, ij'k'l'\cdots, ij''k''l''\cdots, \cdots)$ are connected at each vertex (see Figs. 3~5). The density matrices of the vertex i , $\rho^{(1)}(\sigma_i)$, and that of the cluster $ijkl\cdots$, $\rho_{ijkl\cdots}^{(c)}$, are given by²²⁾ (superscripts 1 and c stand for one-body and cluster, respectively)

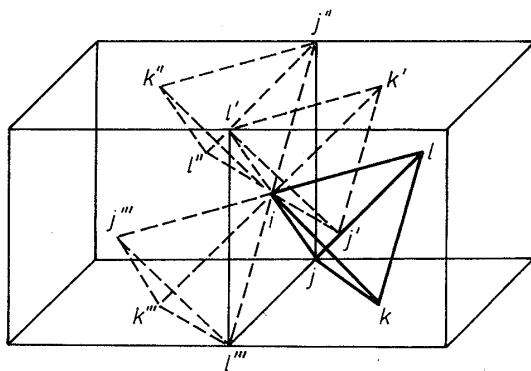


Fig. 3. Face-centered cubic lattice.

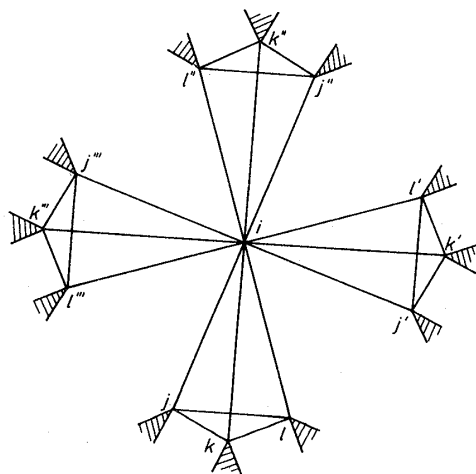


Fig. 4. Tetrahedron cactus lattice.

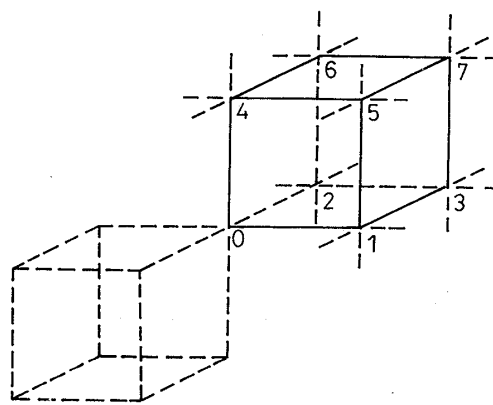


Fig. 5. Cube cactus lattice.

$$\rho_i^{(1)} = \rho^{(1)}(\sigma_i) = \exp(\beta H_i^{(1)} \sigma_i) \tag{4.1}$$

$$= A^{(1)}(1 + l_i^{(1)} \sigma_i), \tag{4.1'}$$

$$\rho_{ijkl\dots}^{(c)} = \rho^{(c)}(\sigma_i, \sigma_j, \sigma_k, \dots) = \exp(\sum_{\mu\nu} \beta J_{\mu\nu} \sigma_\mu \sigma_\nu + \sum_{\mu} \beta H_{\mu}^{(c)} \sigma_{\mu}) \tag{4.2}$$

$$= A^{(c)} \prod_{\mu\nu} (1 + t_{\mu\nu} \sigma_\mu \sigma_\nu) \prod_{\mu} (1 + l_{\mu} \sigma_{\mu}), \tag{4.2'}$$

where

$$t_{\mu\nu} \equiv \text{th } \beta J_{\mu\nu}, \quad l_{\mu}^{(1)} \equiv \text{th } \beta H_{\mu}^{(1)}, \quad l_{\mu} \equiv \text{th } \beta H_{\mu}^{(c)}.$$

$H_i^{(1)}$ is the effective field at the site i contributed from all the clusters connected at the site i . $H_i^{(c)}$ (which should be written as $H_{i-ijkl\dots}^{(c)}$) is the effective field at the site i contributed from the outside of the cluster $ijkl\dots$, and $\mu\nu$ in $\sum_{\mu\nu}$ and $\prod_{\mu\nu}$ runs over all the connected bonds of the cluster $ijkl\dots$, and μ in \sum_{μ} and \prod_{μ} runs over all the vertices of the cluster. We postulate that the physical quantities obtained from the one-body density matrix and those from the cluster density matrix should be equal. Then it leads to the following reducibility of the normalized density matrices:

$$\text{tr}_{ijkl\dots} \tilde{\rho}_{ijkl\dots}^{(c)} = \tilde{\rho}_i^{(1)}.$$

The condition holds rigorously for the cactus lattice considered here. $\text{tr}_{ijkl\dots} \rho_{ijkl\dots}^{(c)}(\sigma_i, \sigma_j, \sigma_k, \dots)$ is a linear function of σ_i and has the form

$$\sum_{\sigma_j \sigma_k \dots} \rho_{ijkl\dots}^{(c)}(\sigma_i, \sigma_j, \sigma_k, \dots) = A^{(c)} \exp[(\beta H_i^{(c)} + \beta h_{i-ijkl\dots}) \sigma_i]. \tag{4.3}$$

Substituting $\sigma_i = \pm 1$ into (4.3), we have

$$h_{i-ijkl\dots} = (1/2\beta) \ln[f(1)/f(-1)], \tag{4.4}$$

where

$$f(\sigma_i) \equiv \sum_{\sigma_j \sigma_k \dots} \exp(-\beta H_i^{(c)} \sigma_i) \rho_{ijkl\dots}^{(c)}(\sigma_i, \sigma_j, \sigma_k, \dots), \tag{4.5}$$

$h_{i-ijkl\dots}$ is the effective field at the site i contributed from the inside of the cluster $ijkl\dots$ (single-cluster effective field). Since

$$H_i^{(1)} = h_{i-ijkl\dots} + h_{i-ij'k'l'v\dots} + h_{i-ij''k''l''v''\dots} + \dots, \tag{4.6}$$

we have

$$H_{i-ijkl\dots}^{(c)} = H_i^{(1)} - h_{i-ijkl\dots}. \tag{4.7}$$

The distribution of the exchange energy J_{ij} results in the distribution of the effective fields $H_i^{(1)}$, $H_{i-ijkl\dots}^{(c)}$ and $h_{i-ijkl\dots}$. We denote these distribution functions by $G^{(1)}(H_i^{(1)})$, $G^{(c)}(H_{i-ijkl\dots}^{(c)})$ and $g(h_i)$, respectively. From (4.6) and (4.7) we have

$$G^{(1)}(H_i^{(1)}) = \int \delta(H_i^{(1)} - h_{i-ijkl\dots} - h_{i-ij'k'l'v\dots} - h_{i-ij''k''l''v''\dots} - \dots) \times \prod_{\mu\nu} P(J_{\mu\nu}) dJ_{\mu\nu} \prod_{\mu} G^{(c)}(H_{\mu}^{(c)}) dH_{\mu}^{(c)}, \tag{4.8}$$

$$G^{(c)}(H_{i-ijkl\dots}^{(c)}) = \int \delta(H_{i-ijkl\dots}^{(c)} - h_{i-ij'k'l'v\dots} - h_{i-ij''k''l''v''\dots} - \dots) \times \prod_{\mu\nu} P(J_{\mu\nu}) dJ_{\mu\nu} \prod_{\mu} G^{(c)}(H_{\mu}^{(c)}) dH_{\mu}^{(c)}. \tag{4.9}$$

The numbers of h in the δ -function in (4.8) and (4.9) are z_c and $z_c - 1$, respectively. $\mu\nu$ in $\prod_{\mu\nu}$ takes all the connected bonds in the clusters $ijkl\cdots, ij'k'l'\cdots, ij''k''l''\cdots, \cdots$. μ in \prod_{μ} takes all the vertices of clusters $ijkl\cdots, \cdots$ except i . \prod' excludes the cluster $ijkl\cdots$. Since \prod in (4.9) can be grouped in separate clusters, the Fourier transform can be used and we have

$$G^{(c)}(H_i^{(c)}) = \frac{1}{2\pi} \int dx \exp(ixH_i^{(c)}) [S(x)]^{z_c-1}, \tag{4.10}$$

$$S(x) = \int \exp(-ixh_{i-ijkl\cdots}) \prod_{\mu\nu} P(J_{\mu\nu}) dJ_{\mu\nu} \prod_{\mu} G^{(c)}(H_{\mu}^{(c)}) dH_{\mu}^{(c)}, \tag{4.11}$$

where μ in \prod_{μ} runs over the vertices of one cluster $ijkl\cdots$ except i , and $\mu\nu$ in $\prod_{\mu\nu}$ runs over the connected bonds in the cluster. Once the solution of the integral equation (4.10) is obtained, the distribution function of the one-body effective field is given by

$$G^{(1)}(H^{(1)}) = \frac{1}{2\pi} \int \exp(ixH^{(1)}) [S(x)]^{z_c} dx \tag{4.12}$$

and the magnetization σ and the spin glass order parameter q by the same equations as (2.13) and (2.14).

It is noted that the integral equation of the distribution function can be derived by the stationarity of the free energy in the cumulant expansion^{16),22)} in general.

§ 5. Transition temperatures in the cluster approximation

The integral equation (4.10) with (4.11) has a solution $g(h) = \delta(h)$ ($G^{(c)}(H^{(c)}) = \delta(h^{(c)})$) at all temperatures, and it describes the paramagnetic state. (4.10) with (4.11) has another solution in which $\overline{l}_i \neq 0$ and still another in which $\overline{l}_i = 0$ but $\overline{l}_i^2 \neq 0$ in respective temperature regions ($l_i \equiv \text{th} \beta H_i^{(c)}$). The temperatures at which the first and second solutions begin to appear, are the Curie temperature T_c and the spin glass transition temperature T_g , respectively.

In such lattices as the square, hexagonal, simple cubic, body-centered cubic \cdots lattices, where the lattice can be divided into two equivalent sublattices, the cluster approximation gives a quantitative improvement. For example for the cube cluster (Fig. 4), $f(\sigma_0)$ given by (4.5) takes the form²³⁾

$$\begin{aligned} f(\sigma_0) = & \sum_{\sigma_1 \sigma_2 \cdots \sigma_7} (1 + l_1 \sigma_1)(1 + l_2 \sigma_2)(1 + l_3 \sigma_3)(1 + l_4 \sigma_4) \\ & \times (1 + l_5 \sigma_5)(1 + l_6 \sigma_6)(1 + l_7 \sigma_7)(1 + t_{01} \sigma_0 \sigma_1)(1 + t_{13} \sigma_1 \sigma_3)(1 + t_{32} \sigma_3 \sigma_2) \\ & \times (1 + t_{30} \sigma_3 \sigma_0)(1 + t_{04} \sigma_0 \sigma_4)(1 + t_{15} \sigma_1 \sigma_5)(1 + t_{26} \sigma_2 \sigma_6)(1 + t_{37} \sigma_3 \sigma_7)(1 + t_{45} \sigma_4 \sigma_5) \\ & \times (1 + t_{57} \sigma_5 \sigma_7)(1 + t_{76} \sigma_7 \sigma_6)(1 + t_{64} \sigma_6 \sigma_4). \end{aligned} \tag{5.1}$$

Carrying out the summation with respect to σ_i is an appropriate example of the REDUCE program. The result of (5.1) is written in the form

$$f(\sigma_0) = A_0 + \left(\sum_{i=1}^7 B_i l_i \right) \sigma_0 \tag{5.2}$$

and the transition temperatures are given by

$$\sum_{i=1}^7 \overline{(B_i/A_0)^n} = \frac{1}{z_c - 1}. \tag{5.3}$$

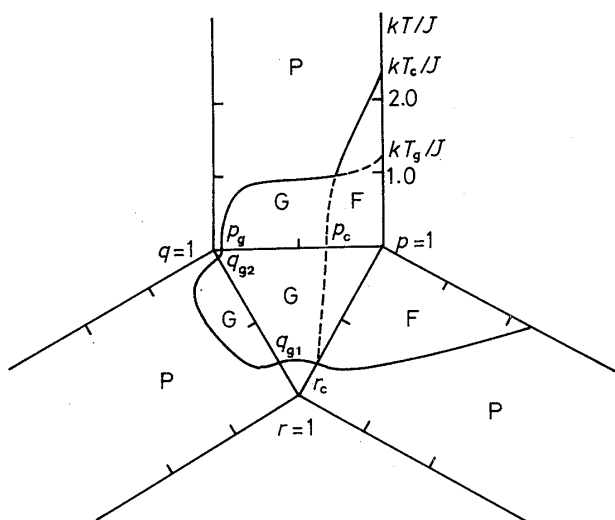


Fig. 6. Phase diagram of the system in the triangular lattice (Random mixture of ferromagnetic, antiferromagnetic and nonmagnetic bonds).²²⁾

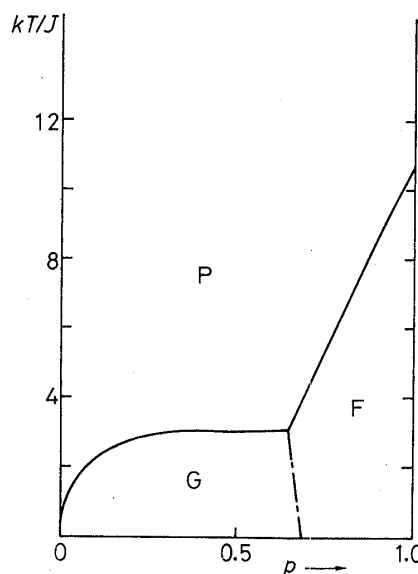


Fig. 7. Phase diagram of the system in the fcc lattice.²⁶⁾ $p_{FG}=0.682$.

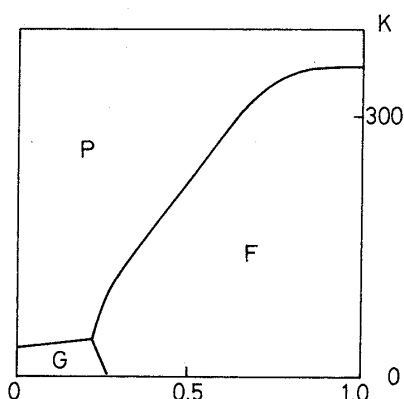


Fig. 8. Phase diagram of $(Cr_{1-y}V_y)_{1-\delta}Te$ (from Ohta, Kurosawa and Anzai²⁷⁾).

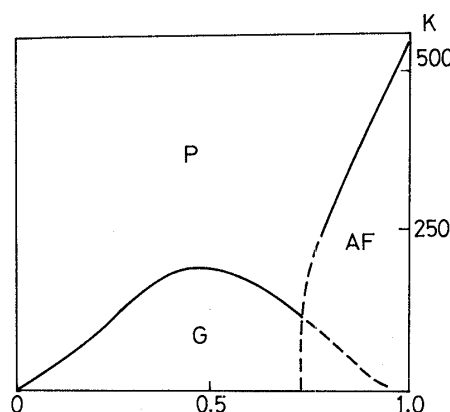


Fig. 9. Phase diagram of Mn_pCu_{1-p} (from Gibbs and Smith²⁸⁾).

Explicit forms of A_0 and B_i and the phase diagram are given in Ref. 23).

As stated in the previous section, the cluster approximation gives qualitatively different results for lattices which cannot be divided into two equivalent sublattices. Examples are the kagome,²⁴⁾ triangular²²⁾ and face-centred cubic lattices^{25),26)} (tetrahedron approximation). Figure 6 shows the phase diagram of the model with ferromagnetic, antiferromagnetic and nonmagnetic bonds [$P(J)=p\delta(J-J_0)+q\delta(J+J_0)+r\delta(J)$, ($p+q+r=1$)]. Figure 7 shows the phase diagram of the system on the fcc lattice. The result in Fig. 7 resembles qualitatively to experiments^{27),28)} for $(Cr_pV_{1-p})_{1-\delta}Te$ and Mn_pCu_{1-p} (Figs. 8 and 9) and others.

§ 6. The boundary between the spin glass and ferromagnetic states and the ground state energy and entropy

We consider the distribution function at $T=0$ and $H=0$. First the pair approximation is treated.⁶⁾ When $T \rightarrow 0$, we see that

$$\lim_{\beta \rightarrow \infty} \frac{1}{\beta} \text{th}^{-1}(\text{th} \beta x \text{ th} \beta y) = \text{sgn}(x) \text{sgn}(y) \min(|x|, |y|). \quad (6 \cdot 1)$$

We assume that at $T=0$ the distribution of the single-cluster effective field is given by a superposition of three delta functions:

$$g(h) = \sum_{n=-1}^1 a_n \delta(h - nJ), \quad (6.2)$$

i.e.,

$$S(x) = \sum_n a_n \exp(-inJx). \quad (6.2')$$

Substituting (6.2) into (2.6) we have

$$G^{(2)}(H^{(2)}) = \sum_m b_m \delta(H^{(2)} - mJ) \quad (6.3)$$

for the distribution function of the two-body effective field $H^{(2)}$. b_n is given by the coefficient of ξ^n in the expansion of $(\sum a_n \xi^n)^{z-1}$. Inserting (6.3) into (2.7) with (6.1) we have new $S(x)$ as

$$S(x) = \sum_n a_n' \exp(-inJx). \quad (6.4)$$

a_n' is expressed in terms of b_m and b_m in terms of a_n . Hence we have algebraic equations for a_n . The values which satisfy these relations give a solution of the integral equation. The solutions are classified in the following types. A single peaked δ -function at $h=0$ describes the paramagnetic state. An asymmetric solution describes the ferromagnetic state. A symmetric solution with nonzero width describes the spin glass state. The value of the concentration of the ferromagnetic bond where the asymmetric solution begins to appear, and connects with the symmetric solution, p_{FG} , is the phase boundary between the ferromagnetic and spin glass states at $T=0$.

For $z=3$ (hexagonal lattice) we have

$$\begin{aligned} a_0 &= (a_0^2 + 2a_{-1}a_1), \\ a_1 &= (a_1^2 + 2a_0a_1)p + (a_{-1}^2 + 2a_0a_{-1})(1-p), \\ a_{-1} &= (a_{-1}^2 + 2a_0a_{-1})p + (a_1^2 + 2a_0a_1)(1-p), \end{aligned} \quad (6.5)$$

where p is the concentration of the ferromagnetic bond. (6.5) has three solutions:

$$\text{i) } a_0=1, \quad a_1=a_{-1}=0, \quad (\text{paramagnetic, P}) \quad (6.6)$$

$$\text{ii) } a_0=a_1=a_{-1}=1/3, \quad (\text{spin glass, SG}) \quad (6.7)$$

$$\text{iii) } a_0=2(1-p)/(2p-1),$$

$$a_1 - a_{-1} = \frac{[(8p-7)(4p-3)]^{1/2}}{(2p-1)}. \quad (\text{ferromagnetic, F}) \quad (6.8)$$

The ferromagnetic solution (6.8) disappears at $p_{FG}=7/8$ and connects with the spin glass solution (Fig. 2).

Substituting these values of a_n in (6.7) into (3.9) and (3.10) and pick up the leading two terms, we obtain²⁹⁾ the ground state energy E and entropy S of the spin glass state:

$$E = \frac{23}{27} E_F = 0.85185 E_F,$$

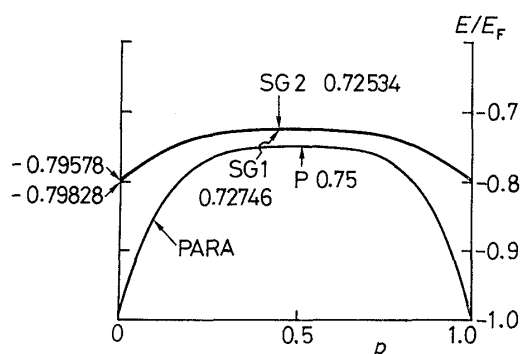


Fig. 10. Ground state energy of the system in the square lattice.³⁰⁾

$$S/k_B = -\frac{11}{54} \ln 2 + \frac{8}{54} \ln 3 = 0.0215607,$$

where $E_F = -\frac{1}{2} zJ$ is the ferromagnetic ground state energy.

For the case $z=4$ (square lattice), we have two spin glass states⁷⁾ SG1 and SG2, and $E_1 = (3/4)E_F$, $S_1/k_B = 0.098108$ for SG1, $E_2 = (93/125)E_F = 0.744E_F$, $S_2/k_B = 0.0390764$ for SG2. The entropies for $z=3$, for SG1 of $z=4$, and for SG2 of $z=4$, are all small positive quantities, in contrast to the negative entropy of infinitely long-ranged model.²⁾ The energy in the paramagnetic state in this approximation, however, is $-J$, and it is lower than that of the spin glass state. $p_{FG1} = 5/6$ and $p_{FG2} = 0.8205$. The situation is much improved by using a square cluster approximation (see below).

We consider a square cactus lattice of $z_c=2$ as an approximation of the square lattice.^{30),31)} For $z_c=2$, a_n is equal to b_n . Substituting $S(x) = \sum_{l=-2}^2 a_l \exp(-ilJx)$ into the integral equation we have algebraic equations for a_n . They are solved as a function of $x \equiv p - 1/2$, and give relevant solutions: 1) P state. $a_0=1$ in the whole region of x . 2) SG1 state. 3) SG2 state. 4) F1 state. $0.335 < |x| < 0.5$. 5) F2 state. $0.327 < |x| < 0.375$. SG1 and F1 connect at $p_{FG1} = 0.835$ with each other, and SG2 and F2 at $p_{FG2} = 0.827$.

The energies and entropies of the spin glass states in the square approximation depend on p while they do not in the pair approximation. Figure 10 shows the ground state energy. The energy of the SG1 and SG2 are very close throughout the whole range. Though the energy of the paramagnetic state is still lower than that of the spin glass state, the former has become close to the latter. This fact suggests that the spin glass energy may become lower than that of the paramagnetic state as the degree of approximation is improved.

We also applied the method to the face-centered cubic lattice in the tetrahedron approximation.^{25),26)} The number of unknowns a_n is 4, but each equation corresponding to (6.5) has 2500-7500 terms on the right-hand side. Figure 11 shows the behavior of the a_n for various values of the concentration of the ferromagnetic bonds p . We see the changes: spin glass \rightarrow ferromagnet \rightarrow pure ferromagnet, as $p = 0.64 \rightarrow 0.9 \rightarrow 1.0$. The boundary between the ferromagnetic and spin glass states, $p_{FG} = 0.682$, was obtained. The phase diagram, shown in Fig. 8, is consistent with experiments on the fcc spin glass.

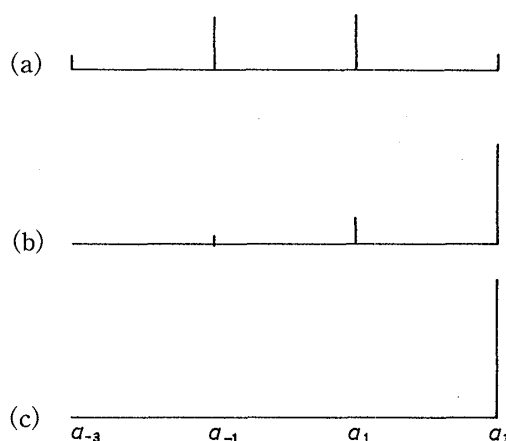


Fig. 11. The solution of the integral equation, a_n , for the fcc lattice at $T=0$. (a) $p=0.64$ (spin glass), (b) $p=0.9$ (ferromagnetic), (c) $p=1.0$ (pure ferromagnetic).²⁶⁾

The one-dimensional problem at $T=0$ with the external field H is exactly solved and the stepwise magnetization process is obtained.³²⁾

§ 7. The site-random Ising model, a model for $\text{Eu}_p\text{Sr}_{1-p}\text{S}$, and other models

Hitherto we treated the spin glass in the bond-random Ising model. Our method can be extended to the site-random Ising model of A and B , of which the exchange integrals are J_{AA}, J_{BB} , and J_{AB} , and the uniform, staggered and spin glass susceptibilities have been obtained in Ref. 33). The transition temperatures are given by

$$1 \mp (z-1)(p_A t_{AA}^n + p_B t_{BB}^n) + (z-1)^2 p_A p_B (t_{AA}^n t_{BB}^n - t_{AB}^n t_{BA}^n) = 0, \tag{7.1}$$

where $t_{AB} \equiv \text{th} \beta J_{AB}$, etc. Upper and lower signs with $n=1$ give the Curie and Néel temperatures, respectively. Upper sign with $n=2$ gives spin glass transition temperature.

The result is extended to a system with second neighbor interactions.³⁴⁾ It was shown that when a proper second neighbor interaction which enhances frustrations exists, the spin glass state becomes easy to appear. Related glass experiments are those for $\text{Eu}_{1-p}\text{Gd}_p\text{S}$, $\text{Fe}_p\text{Cr}_{1-p}$, etc.³⁵⁾

$\text{Eu}_p\text{Sr}_{1-p}\text{S}$ is a crystal in which Eu or Sr forms a fcc lattice and $J_{\text{Eu-Eu}}$ is ferromagnetic or antiferromagnetic when Eu-Eu pair is of first or second neighbors, and $J_{\text{Eu-Sr}}$ and $J_{\text{Sr-Sr}}$ are always zero, and it

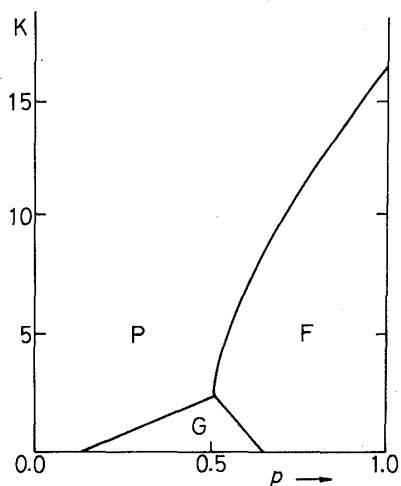


Fig. 12. Phase diagram of $\text{Eu}_p\text{Sr}_{1-p}\text{S}$ (from Maletta and Felsch³⁶⁾).

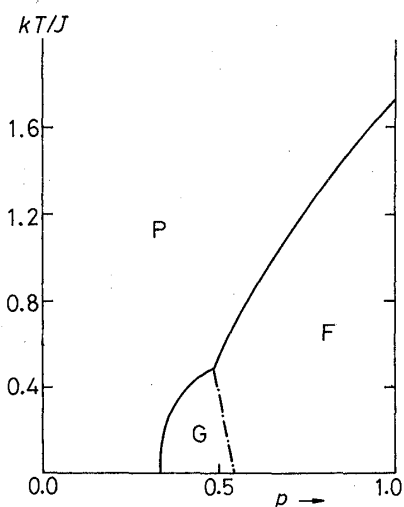


Fig. 13. Phase diagram^{37),38)} of $\text{Eu}_p\text{Sr}_{1-p}\text{S}$.

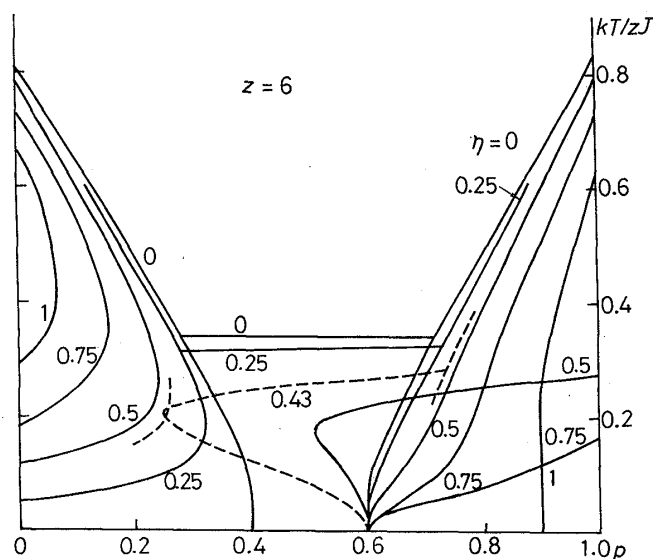


Fig. 14. Phase diagram of the random Heisenberg-Ising model.⁴⁰⁾ When $0.43 < \eta < \eta_c$, the paramagnetic state does not disappear for some region of p as $T \rightarrow 0$. When $\eta < \eta_c$ the spin glass does not appear.

shows the phase diagram³⁶⁾ as in Fig. 12. The theoretical phase diagram^{37),38)} in a site model with first and second neighbor interactions by the square approximation (Fig. 13) is in a qualitative agreement with experiments.

The method in the pair approximation was applied to the classical planar spin glass,³⁹⁾ classical Heisenberg spin glass, and quantum Heisenberg-Ising spin glass.⁴⁰⁾ The Curie, Néel and spin glass transition temperatures for the classical systems are then given by (3·7) and (7·1) if $\text{th}(\beta J)$ are replaced by $I_1(\beta J)/I_0(\beta J)$ and $L(\beta J)$, respectively. Here $I_n(x)$ and $L(x)$ are the Bessel function of an imaginary argument and the Langevin function, respectively. It was shown for the quantum system that, when the anisotropic parameter η ($=0$: Ising, $=1$: isotropic Heisenberg) exceeds a critical value η_c , the spin glass disappears (Fig. 14).

It was shown that Sherrington-Kirkpatrick's result²⁾ for the infinitely long-ranged model is reproduced⁶⁾ by taking the limit $N \rightarrow \infty$ in the pair approximation with a distribution $P(J)$ such that

$$\int J P(J) dJ = J_0/N, \quad \left(\int J^2 P(J) dJ \right)^{1/2} = J_d/N^{1/2}.$$

The integral equation (2·5) for $T=0$ has been shown exactly to have a paramagnetic solution $g(h) = \delta(h)$, and a spin glass solution $g(h) = [\delta(h+1) + \delta(h) + \delta(h-1)]/3$. Other than the above solution, Inawashiro^{41),42)} showed the solutions which are superpositions of more than three delta functions exist. Morita⁴³⁾ obtained a solution composed of three delta functions and a continuous function by a numerical calculation of a histogram. In § 8 we treat the latter solution analytically.

§ 8. Analytical solution of the integral equation (2·9) at $T=0$ with continuous distribution function¹¹⁾

When $T \rightarrow 0$ the kernel (2·10) of the integral equation (2·9) is simplified with the use of (6·1):

$$\begin{aligned} K(x, y) = & e^{-iyH} \left\{ \int_{-\infty}^{\infty} dJ P(J) \int_{|J|}^{\infty} dH^{(2)} \exp[iy(H^{(2)} - J)] \right. \\ & + \int_{-\infty}^{\infty} dJ P(J) \int_{-\infty}^{-|J|} dH^{(2)} \exp[iy(H^{(2)} + J)] \\ & + \int_0^{\infty} dJ P(J) \int_{-J}^J dH^{(2)} \exp[iy(H^{(2)} - J)] \\ & \left. + \int_{-\infty}^0 dJ P(J) \int_J^{-J} dH^{(2)} \exp[iy(H^{(2)} + J)] \right\} \end{aligned} \quad (8\cdot1)$$

$$\begin{aligned} = & e^{-iyH} \left\{ 2\pi \delta(y) \int_{-\infty}^{\infty} P(J) \cos xJ dJ \right. \\ & - 2 \int_0^{\infty} \frac{\sin(y-x)J}{y} P(J) dJ + \int_{-\infty}^0 \frac{\sin(y+x)J}{y} P(J) dJ \\ & \left. + 2 \int_0^{\infty} \frac{\sin(y-x)J}{y-x} P(J) dJ - \int_{-\infty}^0 \frac{\sin(y+x)J}{y+x} P(J) dJ \right\}. \end{aligned} \quad (8\cdot2)$$

Hereafter we consider the case for $z=3$, $H=0$, of the $\pm J$ model [$P(J) = [\delta(J-1)$

+ $\delta(J+1)]/2]$. Since the distribution function $g(h)$ of the single-bond effective field is an even function, $S(x)$ is even. Hence

$$K(x, y) = 2\pi \cos x \delta(y) - 2 \cos x \frac{\sin y}{y} + \frac{\sin(y-x)}{y-x} + \frac{\sin(y+x)}{y+x}. \tag{8.3}$$

Using the addition theorem of the Bessel functions, we have

$$\frac{\sin(y \mp x)}{y \mp x} = \sum_{n=0}^{\infty} (\pm 1)^n (1+2n) j_n(x) j_n(y), \tag{8.4}$$

where $j_n(x)$ is a spherical Bessel function. Expressing the second term of (8.3) also in terms of the spherical Bessel function, we have

$$K(x, y) = 2\pi \cos x \delta(y) - 2 \cos x j_0(y) + 2 \sum_{n=0}^{\infty} (1+4n) j_{2n}(x) j_{2n}(y). \tag{8.3'}$$

Let $S(x)$ be

$$S(x) = a + b \cos x + \sum_{l=0}^{\infty} c_{2l} j_{2l}(x), \tag{8.5}$$

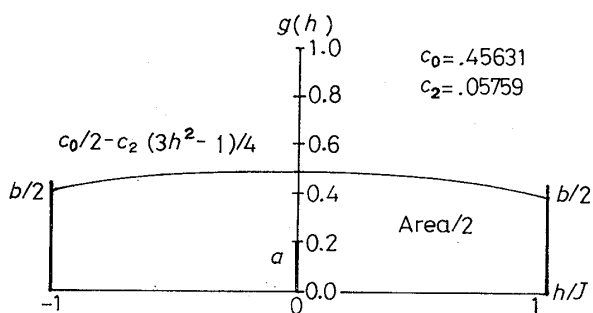
where a, b , and c_{2l} are coefficients to be determined. We substitute (8.3') and (8.5) into (2.9) and integrate the right-hand side. Equating the corresponding coefficients in both sides, we have

$$\begin{aligned} a &= a^2 + b^2/2, \\ b &= 2ab + bc_0 + b^2/2 + c_0^2 - \sum_l \sum_m c_{2l} c_{2m} I_{0,2l,2m}, \\ c_{2n} &= 2ac_{2n} + 2b(1+4n) \sum_l c_{2l} I_{2l,2n} + (1+4n) \sum_l \sum_m c_{2l} c_{2m} I_{2l,2m,2n}, \end{aligned} \tag{8.6}$$

where

$$I_{2l,2m} \equiv \int_{-\infty}^{\infty} dy \cos y j_{2l}(y) j_{2m}(y), \tag{8.7}$$

$$I_{2l,2m,2n} \equiv \int_{-\infty}^{\infty} dy j_{2l}(y) j_{2m}(y) j_{2n}(y). \tag{8.8}$$



Solution: $a = .10683$ $b/2 = .21843$ $\text{Area}/2 = .22816$
 Morita: $a = .10696$ $b/2 = .21854$ $\text{Area}/2 = .22798$

Fig. 15. Distribution of the single-bond effective field in the spin glass state at $T=0$ in the pair approximation.¹¹⁾

We seek a solution where c_4, c_6, \dots are zero. Necessary integrals are calculated to be

$$\begin{aligned} I_{00} &= 1/2, & I_{02} &= 0, & I_{22} &= -7/80, \\ I_{000} &= 3/4, & I_{002} &= 1/16, & I_{022} &= 1/160, \\ I_{222} &= 9/256. \end{aligned} \tag{8.9}$$

Using (8.9), the physically accessible solutions of (8.6) are given by

- i) $a=1, b=0, c_{2n}=0,$
- ii) $a=1/3, b=2/3, c_{2n}=0,$

$$\text{iii) } a=0.10683, \quad b/2=0.21843, \quad c_0=0.45631, \quad c_2=0.05759.$$

The solution i) represents the paramagnetic solution. The solution ii) is the spin glass solution previously obtained. The solution iii) represents a spin glass with a continuous distribution. The values of a , b and c_0 agrees with corresponding quantities of Morita's solution⁴³⁾ with almost 4 valid digits. Rapid damping of I_{mn} and I_{lmn} for indices and the perfect agreement with Morita's results suggests that solutions with nonvanishing c_4, c_6, \dots are very close to the solution now obtained. Figure 15 shows the distribution function $g(h)$ of the single-bond effective field:

$$g(h) = a\delta(h) + \frac{b}{2}[\delta(h+1) + \delta(h-1)] + c_0/2 + c_2(3h^2-1)/4 \quad (|h| < 1+0) \\ = 0. \quad (|h| > 1) \quad (8 \cdot 10)$$

Physical quantities derived from (8·10) are now being calculated.

§ 9. Conclusion and discussion

In this paper the spin glass problem by the method of the distribution function of the effective field developed by our group are reviewed. Reducibility condition between one-body and cluster density matrices leads to an integral equation for the distribution function of an effective field. The solutions of this integral equation are classified into three classes. 1) A single peaked delta function at $h=0$ which represents the paramagnetic state. 2) Symmetric functions with nonzero widths which represent the spin glass states. 3) Asymmetric functions which represent the ferromagnetic state. The antiferromagnetic state is obtained by modifying the integral equation.

The phase boundaries are obtained as a point at which the above solution begins to appear (P-F, P-SG) or connect with each other (SG-F). In the pair approximation of the $\pm J$ model, the phase diagram is symmetric between the ferro- and antiferromagnetic states, between which the spin glass state lies. In the triangle cluster approximation for the triangle or fcc lattice, or in the tetrahedron approximation for the fcc lattice, the antiferromagnetic state does not appear and the phase diagram firstly explains well the experimental results.

The ground state entropies in our results for the short-ranged models are small positive quantities. It is contrary to the appearance of a negative entropy in the infinitely long-ranged model.

A comparison of the ground state energy of the system in the square lattice between the pair and square cactus approximations shows a much improvement in the latter and suggests a possibility that the minimum of the free energy of the spin glass state might be obtained in a more extended cluster approximation.

A spin glass state which has a continuous distribution of an effective field was obtained analytically as a solution of the integral equation. Physical quantities in this state will be reported in the future.

Acknowledgements

The author acknowledges Professor Inawashiro, Professor Morita, Dr. Matsubara, Dr. Fujiki, and all the members in his group, who pushed the present investigation with the author.

References

- 1) S. F. Edwards and P. W. Anderson, *J. of Phys.* **F5** (1975), 965.
- 2) D. Sherrington and S. Kirkpatrick, *Phys. Rev. Lett.* **35** (1975), 1972.
- 3) F. Matsubara and M. Sakata, *Prog. Theor. Phys.* **55** (1976), 672.
- 4) S. Katsura and S. Fujiki, *J. of Phys.* **C12** (1979), 1087.
- 5) T. Morita, *Physica* **98A** (1979), 566.
- 6) S. Katsura, S. Inawashiro and S. Fujiki, *Physica* **99A** (1979), 193.
- 7) S. Inawashiro and S. Katsura, *Physica* **100A** (1980), 24.
- 8) D. J. Thouless, P. W. Anderson and R. G. Palmer, *Phil. Mag.* **35** (1977), 593.
- 9) T. Morita and T. Horiguchi, *Solid State Commun.* **19** (1976), 833.
- 10) S. Katsura and M. Takizawa, *Prog. Theor. Phys.* **51** (1974), 82; **52** (1974), 1075.
- 11) S. Katsura, *Physica*, in press.
- 12) Y. Ueno and T. Oguchi, *J. Phys. Soc. Jpn.* **41** (1976), 1123.
- 13) S. Katsura, *Prog. Theor. Phys.* **55** (1976), 1049.
- 14) S. Fujiki and S. Katsura, *Prog. Theor. Phys.* **65** (1981), 1130.
- 15) M. Suzuki, *Prog. Theor. Phys.* **58** (1977), 1151.
- 16) T. Morita, *J. Math. Phys.* **13** (1972), 115.
- 17) S. Katsura, *Physica* **104A** (1980), 333.
- 18) R. Kikuchi, *Phys. Rev.* **81** (1951), 988.
- 19) R. Kikuchi and H. Sato, *Acta Metall.* **22** (1974), 1089.
- 20) S. Katsura and R. Kikuchi, *Physica* **123A** (1984), 595.
- 21) S. Fujiki and S. Katsura, *J. of Phys.* **C13** (1980), 4723.
- 22) I. Nagahara, S. Fujiki and S. Katsura, *J. of Phys.* **C14** (1981), 3781; **C15** (1982), 3039.
- 23) S. Fujiki, Y. Abe and S. Katsura, *Comp. Phys. Comm.* **25** (1982), 119.
- 24) S. Katsura, *Physica* **88A** (1977), 583; **100A** (1980), 452.
- 25) S. Katsura and I. Nagahara, *J. of Phys.* **C13** (1980), 4995.
- 26) S. Katsura and A. Matsuno, *Physica* **122A** (1983), 483.
- 27) S. Ohta, S. Kurosawa and S. Anzai, *J. Phys. Soc. Jpn.* **51** (1982), 1386.
- 28) P. Gibbs and J. H. Smith, *J. Magn. Magn. Mater.* **15-18** (1980), 155.
- 29) S. Katsura, *Physica* **104A** (1980), 333.
- 30) S. Katsura and I. Nagahara, *Physica* **104A** (1980), 397; **115A** (1982), 300.
- 31) S. Katsura, T. Suenaga and T. Imaizumi, *Physica* **116A** (1982), 368.
- 32) S. Katsura and N. Miyamoto, *Physica* **112A** (1982), 393.
- 33) S. Katsura, S. Fujiki and S. Inawashiro, *J. of Phys.* **C12** (1979), 2839.
- 34) S. Katsura and K. Konishi, *Phys. Stat. Solidi.* **(b) 112** (1982), 399.
- 35) A. Berton, J. Chaussy, J. Odin, R. Rammal, F. Folzberg and S. von Molnar, *J. Appl. Phys.* **52** (1981), 1763.
S. M. Shapiro, C. R. Fincher, Jr., A. H. Palumbo and R. D. Parks, *J. Appl. Phys.* **52** (1981), 1792.
- 36) H. Maletta and W. Felsch, *Phys. Rev.* **B20** (1979), 1245.
- 37) S. Katsura and I. Nagahara, *Z. Phys.* **B41** (1981), 349.
- 38) S. Katsura and A. Matsuno, *Phys. Stat. Solidi* **(b) 119** (1983), 73.
- 39) S. Katsura and T. Shirakura, *Phys. Stat. Solidi* **(b) 113** (1982), 327.
- 40) S. Katsura and T. Shimada, *Phys. Stat. Solidi* **(b) 97** (1980), 663.
- 41) S. Inawashiro, private communication (1980).
- 42) S. Inawashiro et al., to be published.
- 43) T. Morita, *Physica* **125A** (1984), 321.